JOURNAL OF GEOPHYSICAL RESEARCH, VOL. 100, NO. C7, PAGES 13,309–13,320, JULY 15, 1995

The variation in the inherent optical properties of phytoplankton near an absorption peak as determined by various models of cell structure

J. Ronald V. Zaneveld and James C. Kitchen
College of Oceanic and Atmospheric Sciences, Oregon State University, Corvallis

Abstract. Optical oceanography models of attenuation and scattering properties often contain simple spectral relationships. Electromagnetic theory, however, predicts fluctuations in the spectra of the attenuation coefficients and scattering properties of substances at wavelengths near an absorption peak. We have modeled these effects for phytoplankton using homogeneous, two-layered, and three-layered sphere models of cell structure and using a wide range of plausible particle size distributions. The magnitude of the scattering in backward directions is affected the most. The effect on the beam attenuation spectra is relatively small compared with the effect on the absorption and scattering coefficients. The backscattering coefficient shows large variability, varying by almost a factor of 3 for some models. The results suggest that beam attenuation at any wavelength in the red shorter than the wavelength of the chlorophyll absorption peak will be insensitive to the chlorophyll content of the particles. Increases in the pigment content per unit volume of phytoplankton will increase the index of refraction in the infrared and therefore increase the attenuation and scattering coefficients there.

Introduction

The spectral structure of the volume scattering function together with the absorption coefficient (the inherent optical properties (IOP)) and the radiance at the boundary determine the distribution of radiance in the interior of the ocean as well as the radiance that emerges from the ocean. Since optical oceanographers tend to use simple wavelength dependencies (the wavelength dependence of the scattering function is nearly always modeled as λ^{-n}), more complex spectral dependencies should be investigated.

The upwelling radiance just above the sea surface is used by means of remote sensing to determine various particulate properties by inversion. Inversion of radiance data such as obtained using remote sensing involves assumptions regarding the spectral dependence of the IOP on particulate properties. Recent studies have shown that the reflectance as a function of solar zenith angle is a strong function of the angular shape of the volume scattering function [*Gordon*, 1989; *Morel and Gentili*, 1991, 1993]. Nevertheless, in the studies cited and in others it is usually assumed that the angular shape of the particulate volume scattering function is not a function of wavelength. The study of the influence of the particle size distribution and internal structure on the spectral dependence of the volume scattering function shape thus has bearing on the remote sensing reflectance. In particular, if narrow bandwidth, full spectral radiance is observed remotely, the spectral dependence of the inherent optical properties near an absorption peak could potentially be inverted to obtain particulate properties.

It is now possible to measure the absorption and attenuation spectra in situ [*Zaneveld et al.*, 1992; *Moore et al.*, 1992]. By subtraction we can thus also obtain the total scattering spectrum in situ. Inversion of this parameter to obtain particulate properties requires parameterization of their interdependence. In addition, the scattering errors of attenuation meters and reflecting tube absorption meters depend on the angular shape of the volume scattering function. *Zaneveld et al.* [1994] have proposed a method for correcting the scattering error of reflecting tube absorption meters. This method assumes that in the near infrared, measured absorption values are due only to absorption by water and to scattering error. The method will only work if the angular shape of the scattering function is nearly constant as a function of wavelength. The structure of the light scattering and absorption properties of oceanic particles can be modeled using electromagnetic theory. We are interested in finding the structure of these parameters near absorption peaks, as the usual oceanographic models are most likely to be incorrect in those regions.

The light-scattering properties of a particle are modified by the presence of an absorbing substance within the particle. For very large particles, light that is absorbed by the particle is not available to be scattered, and thus scattering is diminished an identical amount, resulting in no change in the attenuation. For very small particles, scattering and absorption are independent. In between the interactions are more complex and increases in absorption can cause either an increase or a decrease in attenuation, depending on the size and index of refraction of the particle. These effects are sometimes called "anomalous diffraction" because they can result in an absorption peak producing an attenuation minimum. The term anomalous diffraction has also been used to denote the complex interference patterns which are modified when the concentration of absorbing material changes, producing diffraction rings with anomalous sizes and brightness [*van de Hulst*, 1957, p. 134]. This process is important in

Paper number 95JC00451.
0148-0227/95/95JC-00451$05.00

particles larger than the wavelength of light with indices of refraction close to that of the surrounding medium. A third use of anomalous diffraction is the approximation to scattering theory which is used for this class of particles. All three meanings refer to roughly the same class of particles. In this paper the first meaning will apply, as we are not interested in diffraction rings per se and we are not using the anomalous diffraction approximation in our calculations.

In the vicinity of the absorption band the index of refraction increases with wavelength, while in other regions it decreases. This process has been called anomalous dispersion [*Jenkins and White*, 1957; *Rossi*, 1957; *van de Hulst*, 1957]. The combination of the anomalous dispersion and anomalous diffraction effects will be the main focus of this paper, since they cause fluctuations in the scattering properties in small intervals of the wavelength regime. In the interest of more accurate nomenclature we will call these effects "absorption peak effects" and drop the adjective "anomalous" when describing the dispersion relationships.

The pigment composition and distribution within a particle thus affect its scattering properties, especially near an absorption peak. In this paper we will address the question of how the angular shape of the volume scattering function varies with wavelength near an absorption peak and how this variation is related to the particle size distribution and the internal distribution of pigment. We will also look at how spectral variations of the volume scattering function affect related properties such as backscattering, attenuation, and reflectance spectra.

The Model

Volume scattering functions in the ocean are strongly peaked in the forward direction due to diffraction by particles larger than the wavelength of light and to inhomogeneities in the refractive properties of water itself due to fluctuations in temperature and salinity. In general, particles that are small relative to the wavelength of light have a more symmetric volume scattering function (VSF) with less of a forward peak in scattering and more backscattering relative to total scattering [*van de Hulst*, 1957; *Ditchburn*, 1963]. Thus the VSF is influenced by the particle size distribution (PSD). The size dependency carries over into the wavelength regime because the size parameter, $\rho = \pi D/\lambda$, is relative to the wavelength which makes particles that are only moderately larger than the wavelength of light scatter more like a large particle in blue light than in red light.

Another parameter that influences the VSF is the index of refraction of the particle. The index of refraction of a substance m as a function of wavenumber ν can be expressed as a complex number, $m(\nu) = n(\nu) - in'(\nu)$, where $n(\nu)$ is the real part of the index of refraction and $n'(\nu)$ is the imaginary part which can be derived directly from the absorption spectrum $a_s(\nu)$ of the substance $a_s n'(\nu) = a_s(\nu)/4\pi\nu$. Absorption bands can be characterized [*Ditchburn*, 1963; *Mueller*, 1974] by damped harmonic oscillators with parameters $\bar{\nu}_j$, f_j, and γ_j, where

$$\bar{\nu}_i = \sum \frac{\varepsilon_{s_i}(\nu)\nu}{\sum \varepsilon_{s_i}(\nu)}$$

is the oscillator wavenumber,

$$f_i = \frac{2303 m_e c_l^2}{N_0 e^2} \int_0^\infty \varepsilon_{s_i}(\nu)\, d\nu$$

is the oscillator strength, and

$$\gamma_i = \frac{2}{\max(\varepsilon_{s_i})} \int_0^\infty \varepsilon_{s_i}(\nu)\, d\nu$$

is the damping coefficient.

Here ε_{s_i} is the molar extinction coefficient for the ith pigment, c_l is the speed of light in a vacuum, N_0 is Avogadro's number, e is unit electron charge, and m_e is the mass of an electron. Given these parameters for the absorption bands in the region of interest, we can get $n(\nu)$ from the Lorentz-Lorenz equations [*Ditchburn*, 1963; *Mueller*, 1974] by solving

$$m^2 - 1 = \frac{Ne^2}{\pi m_e c_l^2} \sum \frac{f_k}{(\bar{\nu}_k^2 - \nu^2) + i\gamma_k \nu} \tag{1}$$

for the real part of the index of refraction. Taking the real part of each side gives

$$n^2(\nu) - n'^2(\nu) - 1 = \frac{Ne^2}{\pi m_e c_l^2} \sum \frac{f_k(\bar{\nu}_k^2 - \nu^2)}{(\bar{\nu}_k^2 - \nu^2)^2 + \gamma_k^2 \nu^2}. \tag{2}$$

Introducing k oscillators in the visible region and n_o^2 for the component of n^2 due to absorption at remote wavelengths and solving for n, we get

$$n(\nu) = \left[n_o^2 + 1 - n'^2(\nu) + \frac{Ne^2}{\pi m_e c_l^2} \sum_{j=1}^{k} \frac{f_j(\bar{\nu}_j^2 - \nu^2)}{(\bar{\nu}_j^2 - \nu^2)^2 + \gamma^2 \nu^2} \right], \tag{3}$$

where n_o^2 is the contribution to n^2 by absorption bands far from the region of interest, and N is Avogadro's number $\times$ 10^{-3}.

Many models assume particles to be internally homogeneous. In reality, particles do not have uniform indices of refraction and absorption properties. They have walls, membranes, and other structures, and their pigment content is contained in a fraction of their volume. As alternative models for some of the structures of oceanic particles, we have employed two- and three-layered spheres [*Kitchen and Zaneveld*, 1992], with the outer shell representing a cell wall or membrane. The middle layer of the three-layered model represents the chloroplasts, and the core represents the cytoplasm or, in the two-layered model, the cytoplasm and chloroplasts. The spherical symmetry has allowed the use of exact solutions [*Mueller*, 1974; after *Kerker*, 1969] of the electromagnetic equations for light scattering. The results of this modeling are in qualitative agreement with observed volume scattering functions. While this model (or indeed any model) is too simple to exactly portray scattering behavior in nature, it does approximate the gross angular distribution of scattering [*Mueller*, 1974; *Kitchen and Zaneveld*, 1992; *Bricaud et al.*, 1992] and thus is appropriate for modeling spectral changes in the overall angular shape of the VSF as opposed to the details of the angular shape itself.

Model Parameters

Phytoplankton Model

Mie theory calculations of volume scattering functions for oceanic particle assemblages have been used extensively in the past [*Pak et al.*, 1971; *Morel*, 1973; *Brown and Gordon*, 1973, 1974]. While it is obvious that details regarding particulate shape are ignored in these calculations, they have nevertheless contributed significantly to our understanding of ocean optics. Much of the accepted thinking about the optical characteristics of phytoplankton is due to homogeneous sphere models [*Bricaud and Morel*, 1986; *Stramski and Kiefer*, 1991]. The present study also suffers from the assumption of sphericity of the particles, but as with the studies before, there are some general trends that can be deduced and there are some conclusions that should direct future experimental work.

We will use the following three different models of phytoplankton: (1) a three-layered concentric sphere model with a high index of refraction outer shell; a high-index, absorbing middle chloroplast layer; and a low index, nonabsorbing core; (2) a two-layered concentric sphere model with a low index outer layer representing the membrane and cytoplasm; and a high index, absorbing inner core representing the central chloroplast; and (3) a homogeneous, medium index, absorbing sphere. Both the real and imaginary components of the index of refraction will be modified in such a way as to make the volume average of both indices over the entire sphere unchanging from model to model.

There is a great deal of natural variation in the relative sizes and indices of refraction of the various cell structures. These variations change the details of the volume scattering function in some ranges of angles [*Kitchen and Zaneveld*, 1992]. Here, however, we are interested only in changes of the general angular shape of the volume scattering function across the visible light spectrum. Thus we have arbitrarily chosen a set of parameters for our three-layered model that produces a volume scattering function generally similar to observed data [*Petzold*, 1972]. These data are widely used for modeling remote sensing and other properties [*Gordon*, 1989; *Morel and Gentili*, 1991, 1993]. The outer shell, representing the cell wall, is assigned an index of refraction of 1.09 (relative to water) with no absorption and a thickness of 5% of the cell radius. The radius of the core is 76% of the radius of the particle. The core is assigned an index of 1.02. Between the core and the outer shell is the chloroplast layer which is assigned a complex index of refraction based on the dispersion calculations and the oscillator parameters given by *Mueller* [1974] with the average real part of the index also at 1.09. This real part will vary slightly spectrally due to the dispersion effect. The oscillator strength has been adjusted proportionally to the pigment concentration per unit volume of chloroplast to account for differences between our model and that of Mueller in structure and total pigment content per cell.

Using particle and pigment data collected at the chlorophyll maximum in the Pacific Central Gyre [*Kitchen and Zaneveld*, 1990] during the Optical Dynamics Experiment (ODEX) [*Pak et al.*, 1986], we computed the chlorophyll concentration within the model chloroplast layer to be 29.4 g L^{-1} which, following *Mueller* [1974], would yield a peak value of $n' = 0.024$. Mueller used a chlorophyll concentration of 50.4 g L^{-1}, but he determined this value for the volume of the chloroplasts themselves, while we disperse the chlorophyll over a larger volume within the cell which we call the chloroplast layer. After adjusting for the changes in pigment concentration, the resulting indices of refraction (see (3)) of the chloroplast layer are as shown in Figure 1. Note that the increase in the real part of the index of refraction to the long-wavelength side of the peak remains after the imaginary part has returned to zero. There is also a local minimum in the real part from several nanometers to 20 nm short of the absorption peak.

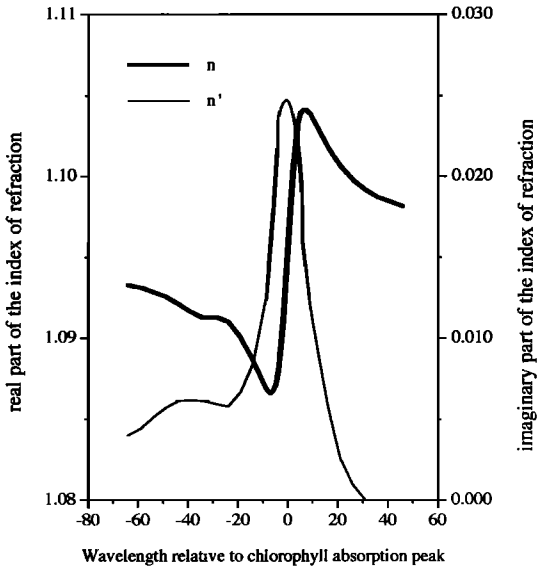

Figure 1. The real and imaginary parts of the index of refraction for the chloroplast layer of a three-layered sphere model of phytoplankton. Chlorophyll content is that inferred from the chloropigment to volume ratio found at the chlorophyll maximum in the Pacific Central Gyre. Wavelengths are differences from that of the absorption peak near 670 nm.

Particle Size Distribution (PSD)

The size distribution of particles in the ocean can generally be described by segmented power laws [*Brown and Gordon*, 1974; *Kitchen and Zaneveld*, 1990] of the form:

$$dN = N_i D^{-S_i} dD, \qquad d_i < D < d_{i+1}. \tag{4}$$

During ODEX, we found PSDs in the Pacific Central Gyre to be characterized by two segments. Particles less than about 6 μm in diameter had a lower exponent than those greater than 6 μm. These exponents varied systematically with depth. For our modeling we will use two PSDs measured in the central gyre and two single-exponent PSDs. The two measured PSDs are averages of the mixed layer PSDs and the average PSD from the pigment maximum. As extreme cases (less realistic), we will use single-exponent models with $s = 3$ and $s = 5$. The former might be representative of a bloom dominated by large diatoms and the latter of a bloom of nanoplankton. These size distributions are shown in Figure 2. All the PSDs have been adjusted to produce the same total particulate volume concentration and thus the same total pigment concentration for the model in this paper.

We have performed the Mie calculations on a Macintosh IIcx computer with limits of integration of 0.5 and 30 μm diameter. That range is all that was practical on that com-

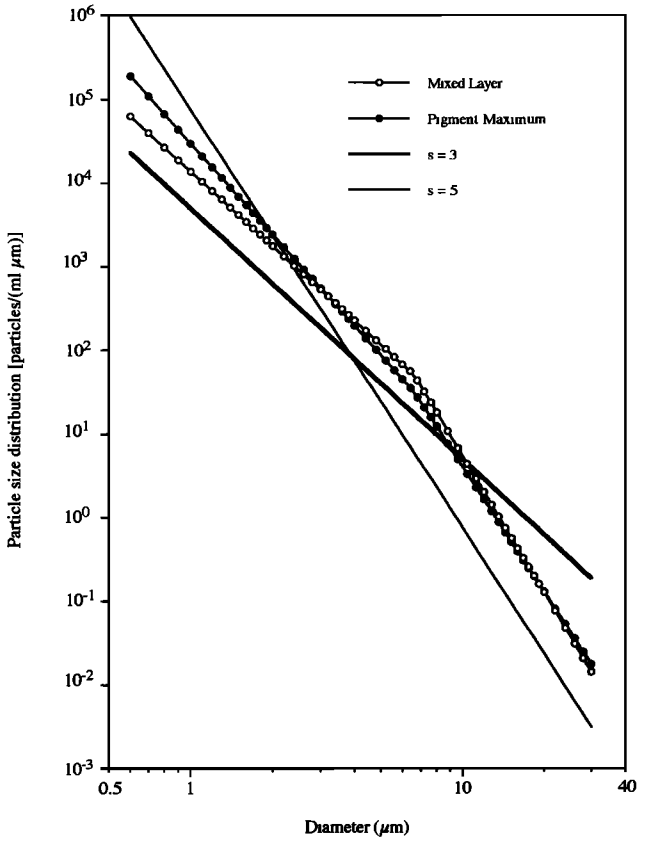

Figure 2. Particle size distributions for the four cases used in the text.

puter for the three-layered sphere FORTRAN code we were using. Subsequently, we have implemented an improved code on a mainframe. The conclusions we drew from an initial test of the improved code were the following. (1) While the small particles (0.2–0.5 μm) added about 20% to the backscattering in the 600- to 715-nm region, they did not contribute significantly to the spectral variability of the various scattering properties. They did, however, bring the volume scattering functions even closer to those observed by *Petzold* [1972] (2) Scattering at angles less than 3° continues to increase as larger and larger particles are included even with the steeply sloped size distributions we were using for them. Thus we will not look closely at the near-forward scattering. This also increases the agreement with Petzold's model, but since particle size distributions are not known to infinity, the problem of near-forward scattering is intractable by this approach. Thus, for the purposes of studying the above described absorption peak effects, we believe the range of 0.5 to 30 μm is adequate and will use the data already generated by the Macintosh. Obviously, for work on other aspects we will need to include the smaller particles. Also, by increasing the total backscattering, the contribution of small particles to backscattering will reduce the effect of the absorption peak effects as a percentage of backscattering.

Results

The volume scattering functions (VSF) at various wavelengths near the red chlorophyll absorption peak which were obtained from our model of the PSD from the pigment maximum layer are shown in Figure 3. The particle volume concentration was increased to yield a chlorophyll concentration of 1.0 μg L^{-1}. All data presented in this paper are for a chlorophyll concentration of 1.0 μg L^{-1}. From Figure 3 it would appear that the dispersion effect is small. However, an enlargement showing the midangle scattering on a linear scale (Figure 3, inset) reveals a significant change in magnitude and angular shape of the VSFs. The coefficient of variation ranges from 4 to 16% at the various angles and averages 9%. This region was shown because of its relative flatness. Similar variability is found in other angular regions (not shown), but it is harder to see because of the steepness of the volume scattering function.

To examine the effect of the internal structure of the particles on the spectral variability of the volume scattering function, we have presented the results of using a homogeneous model (Figure 4) and a model with the chloroplast in the center (Figure 5) surrounded by a low-index (1.02) cytoplasm and membrane. In both of these models the real and imaginary parts of the index of refraction were adjusted to produce the same average indices over the entire particle. Figures 3, 4, and 5 thus represent particle ensembles with the same size distribution and pigment content. We see that the central chloroplast model produces much more variability as a function of wavelength at the intermediate and large angles. The coefficient of variation for this model ranges from 6 to 71% and averages 24%. The homogeneous model produces intermediate results. In nature a mixture of particle structures would be found with the smaller organisms perhaps having simpler structures. Thus we have combined our three structures (Figure 6) into one particle ensemble, with the smaller particles consisting predominantly of homoge-

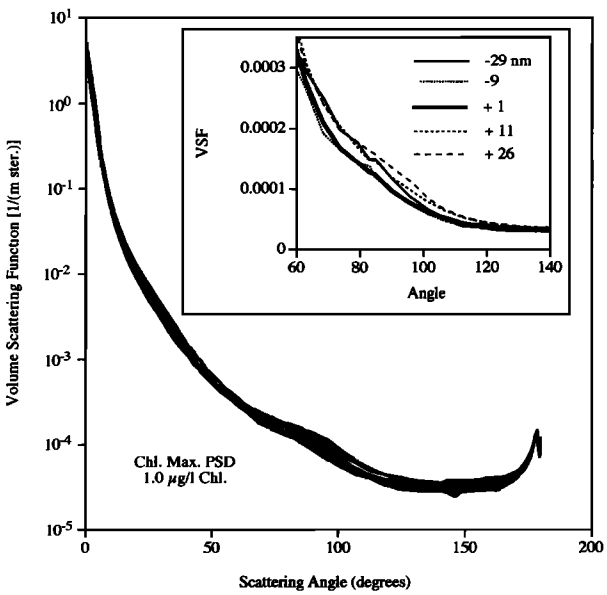

Figure 3. Variations in the volume scattering function with wavelengths from 29 nm short of the absorption peak to 26 nm beyond the absorption peak. The three-layered sphere model of the particles in the chlorophyll maximum layer was used with a total chlorophyll concentration of 1.0 μg L^{-1}. Inset shows a linear enlargement of the volume scattering function in the 60° to 140° range of scattering angles.

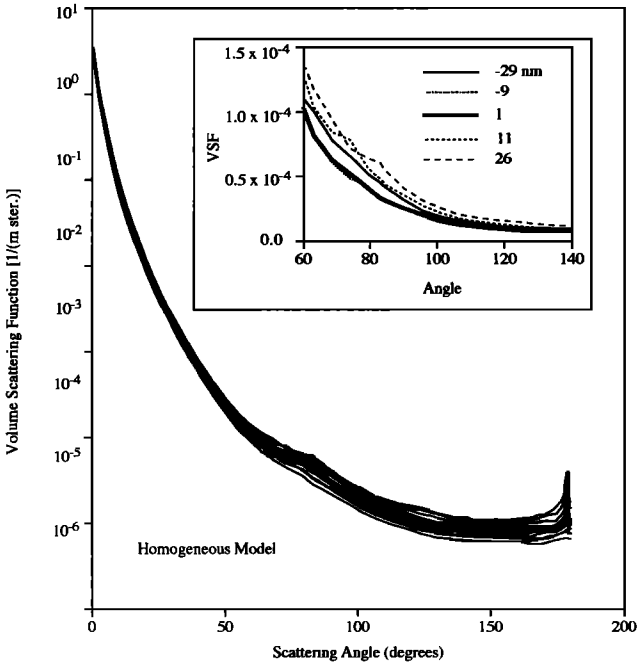

Figure 4. Variations in the volume scattering function with wavelengths from 29 nm short of the absorption peak to 26 nm beyond the absorption peak. The homogeneous sphere model of the particles in the chlorophyll maximum layer was used, with a total chlorophyll concentration of 1.0 μg L^{-1}. Inset shows a linear enlargement of the volume scattering function in the 60° to 140° range of scattering angles.

neous and central chloroplast particles, while the larger particles are modeled as being three-layered. The resulting volume scattering functions are similar in variability (7–28%) and shape to those for the three-layered model but slightly lower in absolute magnitude. Changes in the particle size distribution would cause larger changes (Figure 7) in the shape of the volume scattering function at all angles.

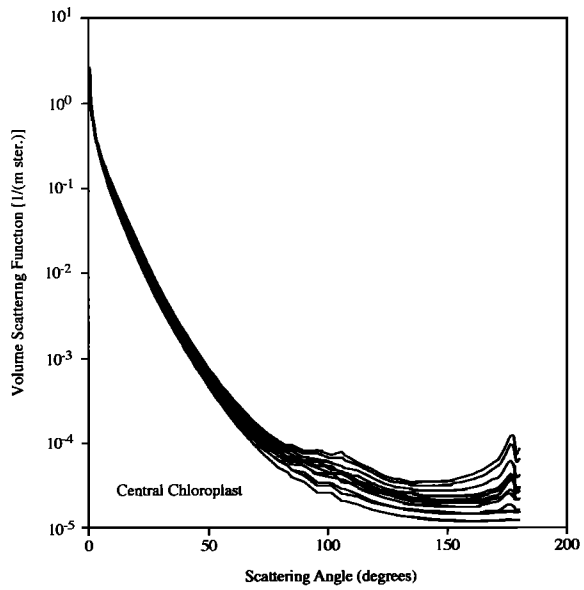

Figure 5. Variations in the volume scattering function with wavelengths from 29 nm short of the absorption peak to 26 nm beyond the absorption peak. The central chloroplast model of the particles in the chlorophyll maximum layer was used, with a total chlorophyll concentration of 1.0 μg L^{-1}.

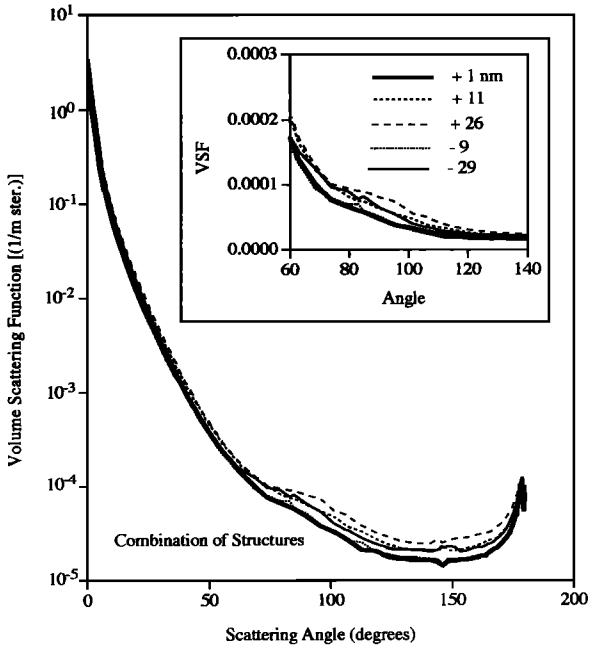

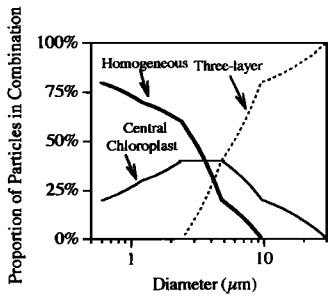

Figure 6. (top) Variations in the volume scattering function with wavelengths from 29 nm short of the absorption peak to 26 nm beyond the absorption peak. A combination of the three models (see bottom diagram for the proportions of each model) was used, with a total chlorophyll concentration of 1.0 μg L^{-1}.

Variations in internal structure do not appear to result in significant changes in the spectra of the attenuation, scattering, or absorption coefficients (Figure 8), but they do cause significant changes in the overall magnitude of attenuation and scattering. There is, however, a significant effect of internal structure on the backscattering spectrum (Figure 9a). The absolute value of the backscattering at a given wavelength for the three-layered sphere model is seen to be more than three times the backscattering for the homogeneous sphere. The magnitude of the backscattering coefficient is obviously also strongly influenced by the relative concentration of small particles. This is seen in Figure 9b, where the $s = 5$ size distribution has b_b values approximately two and a half times those of the $s = 3$ model. The range for the two observed size distributions is much smaller. It thus appears that for the naturally occurring particle ensembles the internal structure has potentially a larger influence on the backscattering than the size distribution.

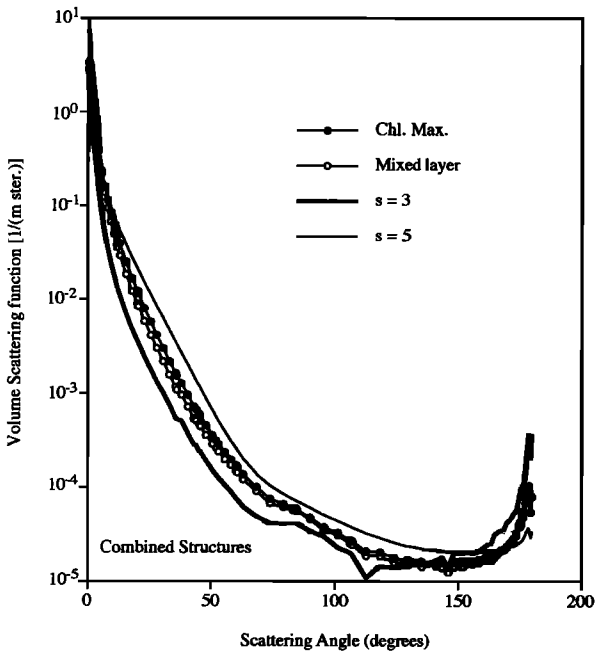

Figure 7. The computed volume scattering functions at the chlorophyll absorption peak for four different particle size distributions using the combination of models.

We also calculated the change in the coefficients when the chlorophyll concentration is increased. The change in attenuation, scattering, and absorption per unit change in chlorophyll concentration within the cell varies very little with cell structure (Figure 10a) except for some self-shading in the absorption spectrum of the central chloroplast model. For wavelengths shorter than the absorption peak the attenuation changes negligibly with chlorophyll. These changes in attenuation would not be discernible from the sample to sample variation for in situ measurements, so that attenuation measurements at wavelengths shorter than 20 nm below the absorption peak are not a function of the pigment concentration. The change in scattering is almost the mirror image of the absorption, but the change in scattering is less dependent on particle structure. However, when the size distributions are changed (Figure 10b), we see much variation in the changes in the coefficients per unit chlorophyll, and the variation is slightly larger for scattering than for absorption. The two observed size distributions produce nearly identical changes in absorption, while the limiting cases of $s = 3$ and $s = 5$ vary by more than a factor of 2.

The spectra of b/a and b_b/a for the particles are shown in Figures 11a and 11b. There is a close agreement between b/a for the two measured size distribution models. The limiting size distribution $s = 3$ and $s = 5$ models show a significant variation in b/a and b_b/a, however. The observed size distributions produce the lowest b/a, since a large portion of the particulate scattering cross section is in the first maximum of the efficiency curve. Here b_b/a varies inversely with the number of small particles due to their high backscattering.

Figures 12a and 12b show spectra of b_b/a with water added. This is approximately three times the irradiance reflectance [*Gordon et al.*, 1975]. Figure 12a indicates that b_b/a increases by approximately 25% when the internal structure of the particles is changed from homogeneous to three-layered. It is seen in Figure 12b that the parameter b_b/a does not vary much as a function of naturally occurring size distributions but that increasing the number of small particles ($s = 5$) increases b_b/a.

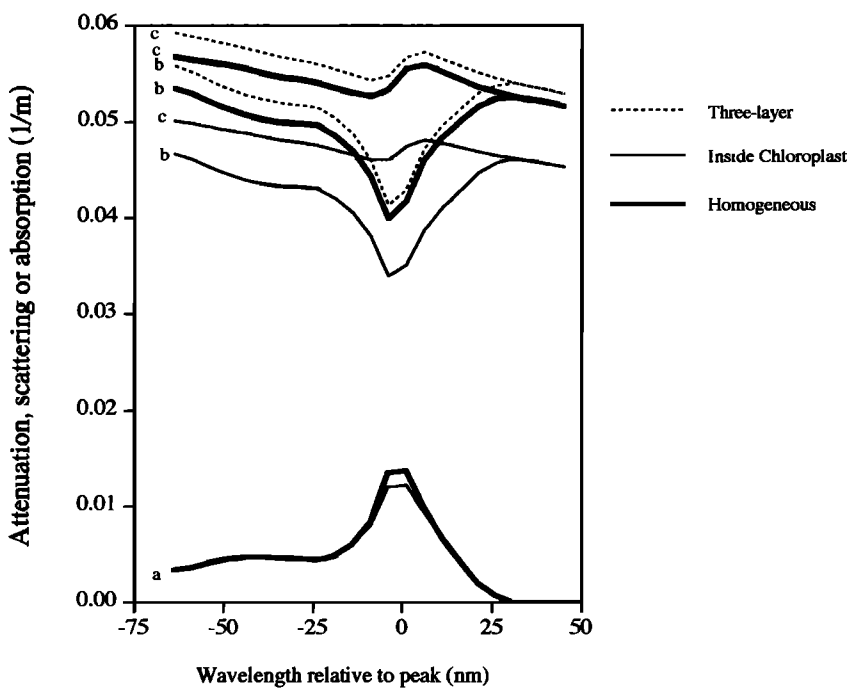

Figure 8. Spectral beam attenuation (lines labeled c), scattering (lines labeled b), and absorption (lines labeled a) coefficients for the three models.

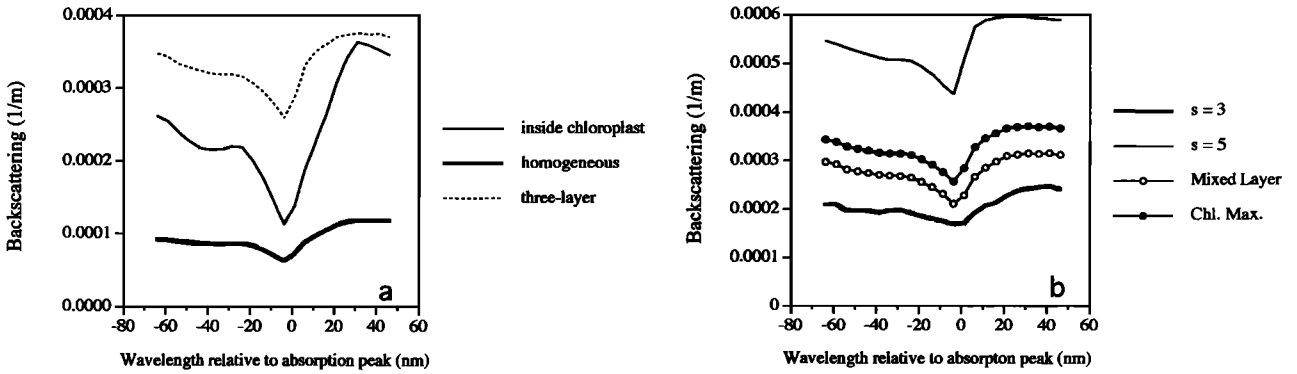

Figure 9. Backscattering spectra for (a) the three models of phytoplankton using the chlorophyll maximum size distribution and (b) the four different size distributions using the three-layered model.

Many optical problems require the portion of scattering that is within some angular range,

$$\frac{2\pi}{b}\int_{\theta_1}^{\theta_2}\beta(\theta,\lambda)\sin\theta\,d\theta.$$

For example, the error in absorption measurements [*Kirk*, 1992; *Zaneveld et al.*, 1992] for water samples contained in glass cells (spectrophotometers or in situ reflective tube absorption meters) is largely due to scattering between some intermediate angle (between 30 and 50°) and 180°. Figure 13 compares the scattering from 30–180° and from 40–180°. The presence of the absorption peak causes variations in the portion of scattering in these ranges of about ±1% of total scattering. The particle size distribution potentially makes a much larger difference if the $s = 5$ limiting case is included. The measured PSDs showed a potential error in the absorption measurements of less than 1% of the total scattering coefficient if the average scattering error is known.

Various integrated ranges of the volume scattering function in the backward direction may be of interest for different remote sensing applications. The particle size distribution is definitely a larger factor in the spectral variation of backscattering (Figure 14) in the ranges of 120–180° and 160–180° than the absorption peak effects if one includes the limiting PSDs. If the particles are predominantly large ($s = 3$), absorption peak effects can cause considerable spectral variation in near 180° scattering.

Discussion and Conclusions

Angular Shape of the Volume Scattering Function

Major variations in the angular and spectral shape of the volume scattering function are due to the size distribution, shape, and internal structure of the particulate population [*Kitchen and Zaneveld*, 1992]. The calculations presented here show that while the particle size distribution has a major influence on the angular shape of the volume scattering function, the influence of the internal structure cannot be ignored.

The effect on remote sensing is due to the large-angle scattering. Both the shape of the scattering function and the magnitude directly affect the reflectance [*Gordon*, 1989; *Morel and Gentili*, 1991; *Zaneveld*, this issue]. At a given angle and a given wavelength the internal structure is seen to cause changes of up to a factor of 3. Since the remote sensing reflectance is proportional to the scattering function at a given angle to within a few percent [*Zaneveld*, this issue], this factor must be taken into account, as we have kept the size distribution and pigment concentration constant in this comparison. The structure and shape of the particles used here are, by definition, not natural. Real phytoplankton are far more complex than we can model. They are, however, highly variable in their internal structure, and some of the effects obtained here are bound to influence real scattering functions. In the backward direction the contribution of the very small particles is important, so that the effects seen here

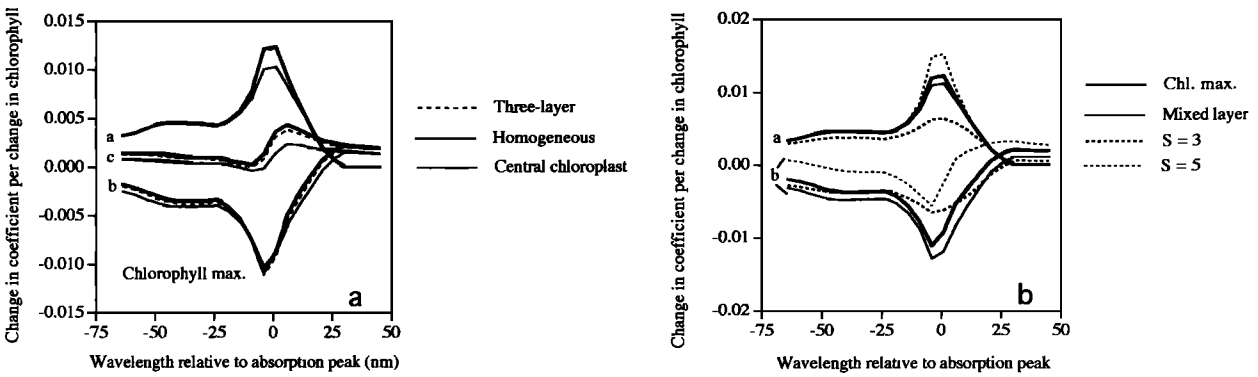

Figure 10. (a) The change in beam attenuation, scattering, and absorption per unit change in chlorophyll content for the three models of phytoplankton. (b) Change in scattering and absorption per unit change in chlorophyll for the four different size distributions using the three-layered sphere model of phytoplankton.

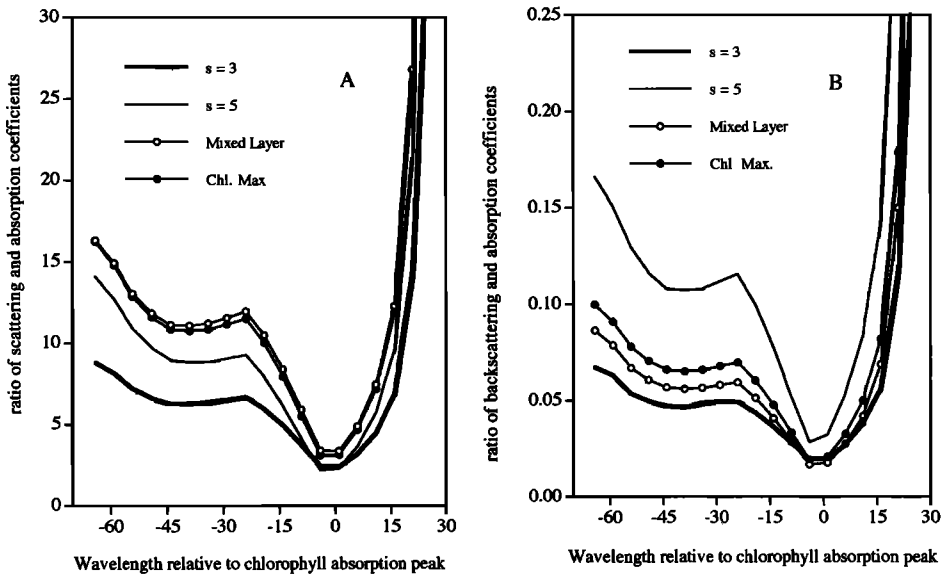

Figure 11. (a) The ratios of the scattering and absorption coefficients and (b) the ratios of the backscattering and absorption coefficients for the four particle size distributions using a three-layered sphere model.

are softened considerably. Experimental work that examines the effect of internal structure on the shape of the volume scattering function is called for.

In addition to the effect of internal structure, there is also a spectral effect due to the presence of an absorption peak beyond that due to the absorption alone. This effect was largest for the model with the central chloroplast (Figure 5). The scattering around 175° is seen to vary by an order of magnitude, depending on wavelength. Scattering at other angles in the backward region still vary by at least a factor of 3. Again, we note that these are models only, but the message is once more that measurements of the scattering function on one side of an absorption peak cannot necessarily be transferred to the other side, without paying some attention to the absorption peak effects.

The near-forward and near-backward scattering seem to have a very strong spectral change in the shape, with greater scattering in those angular regions for shorter wavelengths. The shape of the VSF for intermediate angles has little or perhaps even a reverse general trend for this range of wavelengths.

Influence on Spectral Attenuation and Absorption

Local absorption maxima produce spectral perturbations in the scattering function, with the magnitude of these perturbations dependent on the size distribution of the particles. If we look at the term within the summation of (3), we see that as the wavenumber approaches infinity (wavelength decreases toward zero), the contribution to the index of refraction goes to zero. However, as the wavenumber goes to zero (wavelength increases to infinity), the contribution to the index of refraction squared approaches a positive number [*Rossi*, 1957]

$$\lim_{\nu \to 0} \Delta_j n^2 = \frac{Ne^2 f_j}{\pi m_e c^2 \bar{\nu}_j^2}.$$

The sum of these contributions for all absorption bands over the entire electromagnetic spectrum is the dielectric constant

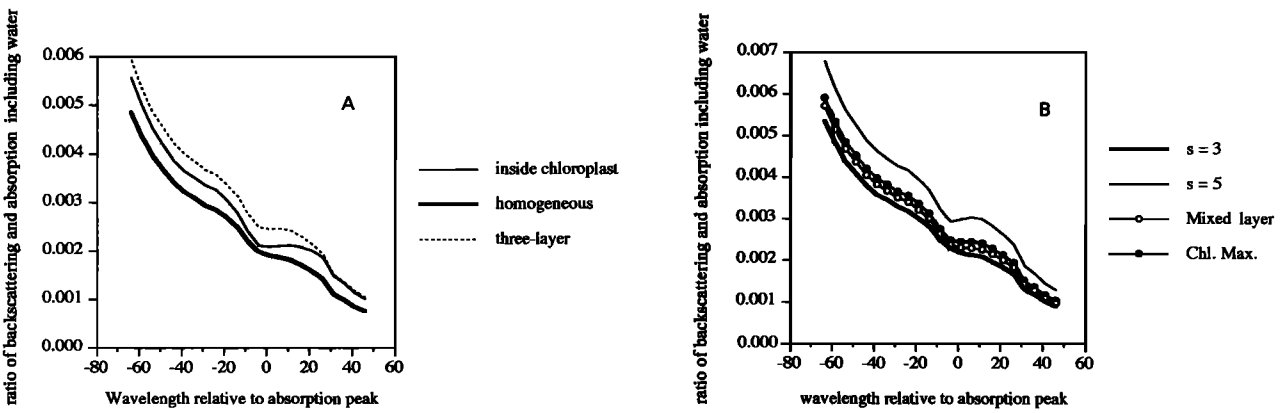

Figure 12. The ratio of the backscattering and absorption coefficients including the contributions of water and for a concentration of 1 μg L^{-1} of chlorophyll for (a) the three models of phytoplankton structure and (b) the four different size distributions using the three-layered model.

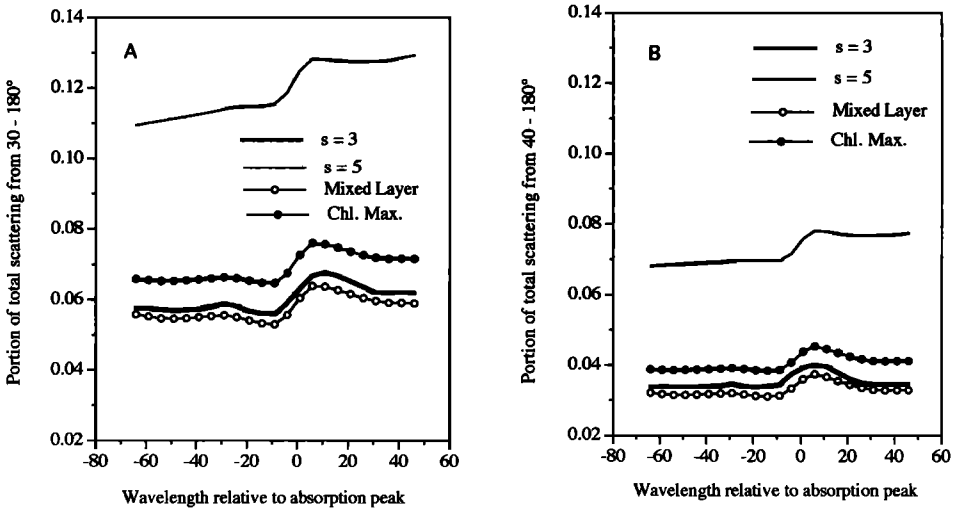

Figure 13. The proportion of the total integrated scattering coefficient that is contained in the intervals (a) 30–180° and (b) 40–180° for each of the four size distributions.

of the substance [*Jenkins and White*, 1957]. Thus an increase in the internal concentration of pigment such as could be due to light adaptation can produce an increase in the particulate index of refraction at all longer wavelengths and thus affect the magnitude and angular shape of the scattering and attenuation spectra. This implies that an increase in the pigment content of the cells will result in increased scattering and attenuation in the green due to the blue peak and in the infrared due to the red absorption peak. The magnitude of this change will, however, depend on the size distribution, and thus the use or removal of this effect to obtain the index of refraction will not be straightforward.

The spectrum of the absorption coefficient was very little influenced by the internal structure (Figure 8), there being only a slight self-shading effect for the inside chloroplast model at the absorption maximum. The absorption spectrum can thus be modeled adequately using homogeneous spheres. In addition, determination of the chlorophyll concentration from the shape of the red absorption peak appears not to be influenced by the internal structure. The shapes of the attenuation and scattering spectra were not affected significantly by internal structure, but the magnitudes were. Beam attenuation values for the inside chloroplast model were about 15% lower than for the three-layered sphere model. The homogeneous model had magnitudes only about 5% below the three-layered sphere model. The shape of the beam attenuation spectra showed a step increase of about 10% when going from the short- to the long-wavelength side of the absorption peak, whereas the scattering coefficient showed a 15% increase. Use of homogeneous spheres for modeling will thus result in errors of ±10% in beam attenuation, which would appear to be acceptable, given the natural variability in the particle concentration of the oceans. A further result is that the inversion of beam attenuation spectra to obtain the particle size distribution [*Shifrin*, 1988], which is based on homogeneous spheres, would appear to be reasonable.

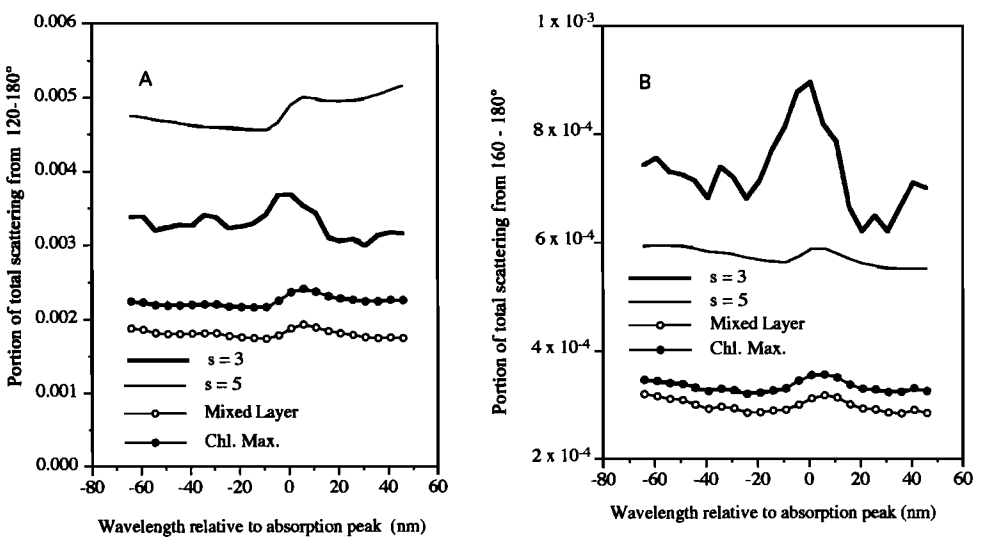

Figure 14. The proportion of the total integrated scattering coefficient that is contained in the intervals (a) 120–180° and (b) 160–180° for each of the four size distributions.

The backscattering spectra (Figure 9a) are far more sensitive to internal structure. The three-layered sphere model gives backscattering coefficients that are about three times as large as the homogeneous spheres. In addition, the shapes of the spectra also vary. Homogeneous sphere models are thus inadequate for the determination of backscattering coefficients [*Bohren and Singham*, 1991]. If one also considers the influence of the geometric shape of the particles, it seems that adequate modeling of backscattering coefficients based on electromagnetic theory is nearly impossible. This emphasizes the need for measurements of this parameter.

Changing the chlorophyll concentration affects the attenuation, scattering and absorption spectra by nearly the same amount, independent of internal structure (Figure 10). The increase in absorption is almost balanced by the decrease in scattering. There is still an effect on the attenuation coefficient. The models seem to indicate that given a size distribution, the step increase in beam attenuation will be proportional to the pigment content. Observations of attenuation (660 nm) per total particle volume concentration and chlorophyll per total particle volume concentration from various coastal and open ocean regions [*Kitchen and Zaneveld*, 1990] have failed to reveal any sensitivity of beam attenuation at 660 nm to the internal chlorophyll content of the particles. This is borne out by the models presented here, in that the change in beam attenuation per unit chlorophyll at wavelengths less than the absorption peak is nearly zero. We have long wondered if this insensitivity to chlorophyll content of the 660-nm transmissometer was due to a fortuitous choice of wavelength, presumably in the scattering minimum of the dispersion curve. However, this effect is only a secondary contributor. The apparent message of Figure 10a is that the insensitivity of the 660-nm transmissometer to chlorophyll concentration is due chiefly to the diffraction effect, and therefore the choice of wavelength is not critical except that wavelengths shorter than the chlorophyll peak will be less sensitive to absorption than those longer than the peak wavelength.

Influence on Remote Sensing Reflectance

In the following discussion we speculate on the influence of the effects calculated here on some remote sensing observations. The reader should once more bear in mind that spherical particle models tend to be unrealistic in a quantitative sense but that the spectral variations calculated here may well exist in nature.

In the vicinity of an absorption peak a fairly large change in the apportionment of attenuation into scattering and absorption can occur. This can produce a change in the reflectance due to phytoplankton alone. The reflectance R is often given as $R = 0.33\ b_b/a$ [*Gordon et al.*, 1975]. Figure 11 shows that the ratio of b_{bp}/a can vary by a factor of 6 when going from 60 nm less than the absorption peak to the wavelength of the absorption peak. This effect is not due only to variations in the absorption coefficient, but, rather, the ratio tends to magnify the opposing spectral variations of scattering and absorption in the neighborhood of an absorption peak. The effect of the particles is obviously muted by the molecular scattering. It would be further reduced by including smaller particles than those covered in this study. If we include molecular scattering in the b_b/a ratio (Figures 12a and 12b), we note that the reflectance can vary by about 20%, depending on the internal structure of the particles. The measured size distributions produce very similar b_b/a spectra, but the $s = 5$ case produces significantly higher values due to the larger proportion of small particles.

The minimum in b_b/a at the absorption peak results in apparent maxima at about 10 nm past the absorption peak. Similar maxima in both shape and magnitude are found in observed reflectance spectra [*Gordon*, 1974; *Roesler and Perry*, this issue]. These peaks are normally attributed to fluorescence. It is interesting that the absorption peak effects described above give very similar looking maxima. Natural fluorescence [*Gordon*, 1979] has been discussed as an indicator of chlorophyll and productivity [*Falkowski and Kiefer*, 1985], and this method for determination of chlorophyll and productivity has been patented [*Booth and Kiefer*, 1989]. However, natural fluorescence at the surface of the ocean shows a surprisingly poor relationship with chlorophyll, especially when a given location is considered [*Roesler and Perry*, this issue]. Natural fluorescence at the surface is not a pure measurement, but it also includes effects of backscattering. As we have seen, there are therefore large effects due to internal structure and size distribution of the particles. We hypothesize that some of the signal attributed to natural fluorescence is due to these absorption peak effects, weakening the direct correlation between chlorophyll and in situ radiance at an absorption peak. This effect needs to be further investigated.

One further result of the potentially increased reflectance due to the effects studied here is that the amount of light emanating from the ocean in the red region of the spectrum may be relatively large. Use of a red channel as a reference for atmospheric corrections in remote sensing must thus be handled with considerable care.

There are some interesting implications of the calculations on the question of the contribution of phytoplankton to the remote sensing reflectance. The water-leaving radiance is proportional to the backscattering [*Gordon and Morel*, 1983; *Zaneveld*, 1982]. The backscattering, at least in case 1 waters, is assumed to be a function of the chlorophyll concentration [*Morel*, 1988], but the phytoplankton are thought to not contribute significantly to the backscattering [*Morel and Ahn*, 1991; *Stramksi and Kiefer*, 1991]. In a way, this is a contradiction, always requiring the nonphytoplankton concentration to be closely related to the chlorophyll concentration. Over large time periods this could be the case, but instantaneously, for example, in plankton blooms, this cannot be true.

Morel and Prieur [1977] noted that absorption spectra computed from remotely sensed data were often below the corresponding absorption spectra calculated from the pigment content and that this discrepancy could be due to a reduction of backscattering by particles in the spectral range where they absorb. This implies that absorbing particles contribute to backscattering. Subsequent papers [*Morel and Ahn*, 1990; *Stramksi and Kiefer*, 1991] have discounted the above contention. In an earlier paper [*Kitchen and Zaneveld*, 1990] we noted that the thickness of the outer layer in the three-layered model has a large influence on the magnitude of the backscattering. In the results described here we note again that the three-layered model gave three times the backscattering of the homogeneous model. We arbitrarily assigned a thickness of 5% of the cell radius to this layer.

M. Orellana and C. Roesler (personal communication, 1993) have discovered that diatoms and dinoflagellates in nature usually have far thicker cell walls than those cultured in the laboratory. They believe this to be the result of environmental stress. If this is the case, the backscattering by phytoplankton could be yet larger than the present three-layered model indicates. A study of the dependence of the thickness of the cell wall on environmental parameters is thus warranted, so that the issue of the contribution of phytoplankton to backscattering can be reexamined.

Applications to Instrumentation

As we have seen, electromagnetic theory produces changes in the shape of the volume scattering function near an absorption peak. As mentioned previously, for calibration of reflecting tube absorption meters we need to know the spectral dependence of the proportion of the scattered light not measured by the absorption meter detector. This proportion for 30 and 40° is shown on Figure 13. The proportion is spectrally far less sensitive than the absolute value of the volume scattering function in the backward direction. We see a variation of about 15% in the proportion, representing less than 1% of the scattering coefficient. Using a near-infrared wavelength to correct for scattering effects in reflecting tube absorption meters should thus lead to error in absorption measurements of the order of 1% of the scattering coefficient.

Except at near-backward angles, changes in the portion of total scattering in any angular range seem to be about 10% of that portion (Figure 14). Most of this observed change occurs at the absorption peak itself. Whether this change is like a step function or an oscillation depends on the size distribution. Farther away, the effect of wavelength on the optical size of the particle might produce larger changes.

Experimental Verification

The actual measurement of $\beta(\theta, \lambda)$ in the field is quite difficult, and when done at all, it is usually at only one wavelength [*van de Hulst*, 1957; *Petzold*, 1972; *Tucker*, 1973] or, at best, a few wavelengths not measured simultaneously [*Pegau et al.*, this issue]. There are thus no measurements of oceanic particle ensembles that we are aware of that could provide us with information regarding the spectral dependence of the angular shape of the volume scattering function close to the chlorophyll absorption peak. We do have experimental information, however, on the spectral shape of the beam attenuation coefficient. *Voss* [1992] described a simple linear equation for the beam attenuation spectra in the open ocean. Upon examination of his table of regressions it is seen, however, that the beam attenuation at 670 nm is, on average, 5.5% higher than the beam attenuation at 630 nm. The 670-nm observations thus contradict the general linear trend. This result makes sense in light of the theoretical scattering calculations. Similar results were obtained by D. A. Siegel (personal communication, 1994) off Bermuda. The beam attenuation spectrum shows a local maximum at 676 nm.

We conclude that these absorption peak effects in the ocean, while in general small, should nevertheless not be ignored. They influence all the IOP to a greater or lesser extent and so must be taken into account if we are to fully understand experimental aspects of ocean optics.

Notation

β the volume scattering function, m^{-1} st^{-1}.
ε_s molar extinction coefficient for a pigment, cm^{-1} mol^{-1}.
γ electromagnetic damping coefficient, cm^{-1}.
λ wavelength of light, nm.
ν wavenumber, cm^{-1}.
θ angle of light scattering, degrees.
ρ particle size parameter, nondimensional.
a absorption coefficient, m^{-1}.
b scattering coefficient, m^{-1}.
b_b backscattering, m^{-1}.
c beam attenuation coefficient, m^{-1}.
c_l speed of light in a vacuum, cm/s.
D diameter of a particle, μm.
e the charge of an electron, C.
f oscillator strength of a pigment absorption band, nondimensional.
m index of refraction, nondimensional.
m_e mass of an electron, g.
n real part of index of refraction, nondimensional.
n' imaginary part of index of refraction, nondimensional.
n_o contribution to index of refraction by absorption bands that are remote from the region of interest, nondimensional.
N_0 Avogadro's number, mol^{-1}.
R reflectance, nondimensional.
s exponent of power law fit to particle size distribution, nondimensional.

Acknowledgments. Support for this research was provided by the Office of Naval Research through grant N00014-90-J-1132 and by the National Science Foundation through grant OCE-8911355.

References

Bohren, C. F., and S. B. Singham, Backscattering by nonspherical particles: A review of methods and suggested new approaches, *J. Geophys. Res.*, *96*, 5269–5277, 1991.

Booth, C. R., and D. A. Kiefer, Method and apparatus for determining concentrations of chlorophyll and the rate of primary production in water, *Pat. 4,804,849*, U.S. Govt. Pat. Off., Washington, D. C., 1989.

Bricaud, A., and A. Morel, Light attenuation and scattering by phytoplanktonic cells: A theoretical modeling, *Appl. Opt.*, *25*, 571–580, 1986.

Bricaud, A., J. R. V. Zaneveld, and J. C. Kitchen, Backscattering efficiency of coccolithophorids: use of a three-layered sphere model, Ocean Optics 11, *Proc. SPIE Int. Soc. Opt. Eng.*, *1750*, 27–33, 1992.

Brown, O. B., and H. R. Gordon, Two component Mie scattering models of Sargasso Sea particles, *Appl. Opt.*, *12*, 2461–2471, 1973.

Brown, O. B., and H. R. Gordon, Size-refractive index distribution of clear coastal water particulates from light scattering, *Appl. Opt.*, *13*, 2874–2881, 1974.

Ditchburn, R. W., *Light*, p. 569, John Wiley, New York, 1963.

Falkowski, P. G., and D. A. Kiefer, Chlorophyll a fluorescence and phytoplankton: Relationship to photosynthesis and biomass, *J. Plankton Res.*, *7*, 715–731, 1985.

Gordon, H. R., Spectral variations in the volume scattering function at large angles in natural waters, *J. Opt. Soc. Am.*, *64*, 773–775, 1974.

Gordon, H. R., Diffuse reflectance of the ocean: The theory of its augmentation by chlorophyll a fluorescence at 685 nm, *Appl. Opt.*, *18*, 1161–1166, 1979.

Gordon, H. R., Dependence of the diffuse reflectance of natural waters on the sun angle, *Limnol. Oceanogr.*, *34*, 1484–1489, 1989.

Gordon, H. R., and A. Morel, *Remote Assessment of Ocean Color for Interpretation of Satellite Visible Imagery*, 114 pp., Springer-Verlag, New York, 1983.

Gordon, H. R., O. B. Brown, and M. M. Jacobs, Computed relationships between the inherent and apparent optical properties of a flat homogeneous ocean, *Appl. Opt.*, *14*, 417–427, 1975.

Jenkins, F. A., and H. E. White, *Fundamentals of Optics*, p. 480, McGraw-Hill, New York, 1957.

Kerker, M., *The Scattering of Light and Other Electromagnetic Radiation*, 666 pp., Academic, San Diego, Calif., 1969.

Kirk, J. T. O., Monte Carlo modeling of the performance of a reflective tube absorption meter, *Appl. Opt.*, *31*, 6463–6468, 1992.

Kitchen, J. C., and J. R. V. Zaneveld, On the noncorrelation of the vertical structure of light scattering and chlorophyll *a* in case I waters, *J. Geophys. Res.*, *95*, 20,236–20,245, 1990.

Kitchen, J. C., and J. R. V. Zaneveld, A three-layered sphere model of the optical properties of phytoplankton, *Limnol. Oceanogr.*, *37*, 1680–1690, 1992.

Moore, C., J. R. V. Zaneveld, and J. C. Kitchen, Preliminary results from an in situ spectral absorption meter data, Ocean Optics 11, *Proc. SPIE Int. Soc. Opt. Eng.*, *1750*, 330–337, 1992.

Morel, A., Diffusion de la lumiere par les euax de mer. Resultats experimentaux et approche theorique, in Electromagnetics of the Sea, *AGARD Lect. Ser.*, *61*(3.1), 1–77, 1973.

Morel, A., Optical modeling of the upper ocean in relation to its biogenous matter content (case I waters), *J. Geophys. Res.*, *93*, 10,749–10,768, 1988.

Morel, A., and Y.-H. Ahn, Optical efficiency factors of free-living marine bacteria: Influence of bacterioplankton upon the optical properties and particulate organic carbon in oceanic waters, *J. Mar. Res.*, *48*, 145–175, 1990.

Morel, A., and Y.-H. Ahn, Optics of heterotrophic nanoglagellates and ciliates: A tentative assessment of their scattering role in oceanic waters compared to those of bacterial and algal cells, *J. Mar. Res.*, *49*, 177–202, 1991.

Morel, A., and B. Gentili, Diffuse reflectance of oceanic waters: Its dependence on Sun angle as influenced by the molecular scattering contribution, *Appl. Opt.*, *30*, 4427–4438, 1991.

Morel, A., and B. Gentili, Diffuse reflectance of oceanic waters, II, Bidirectional aspects, *Appl. Opt.*, *32*, 6864–6879, 1993.

Morel, A., and L. Prieur, Analysis of variations in ocean color, *Limnol. Oceanogr.*, *22*, 709–722, 1977.

Mueller, J. L., The influence of phytoplankton on ocean color spectra, Ph.D. thesis, Oregon State Univ., Corvallis, 1974.

Pak, H., J. R. V. Zaneveld, and G. F. Beardsley, Mie scattering of suspended clay particles, *J. Geophys. Res.*, *76*, 5065–5069, 1971.

Pak, H., D. W. Menzies, and J. C. Kitchen, Optical Dynamics Experiment (ODEX) data report, R/V Acania expedition 10 October–17 November 1982, *Ref. Publ. 86-10*, Coll. of Oceanogr., Oregon State Univ., Corvallis, 1986.

Pegau, W. S., J. R. V. Zaneveld, and K. J. Voss, Toward closure of the inherent optical properties of natural waters, *J. Geophys. Res.*, this issue.

Petzold, T. J., Volume scattering functions for selected ocean waters, *Tech. Rep. 72-78*, Scripps Inst. of Oceanogr., La Jolla, Calif., 1972.

Roesler, C. S., and M. J. Perry, In situ phytoplankton absorption, fluorescence emission, and particulate backscattering spectra determined from reflectance, *J. Geophys. Res.*, this issue.

Rossi, B., *Optics*, p. 365, Addison-Wesley, Reading, Mass., 1957.

Shifrin, K. S., *Physical Optics of Ocean Water*, 285 pp., American Institute of Physics, College Park, Md., 1988.

Stramski, D., and D. A. Kiefer, Light scattering by microorganisms in the open ocean, *Prog. Oceanogr.*, *28*, 343–383, 1991.

Tucker, S. P., Measurements of the absolute volume scattering function for green light in Southern California coastal waters, Ph.D. thesis, Oregon State Univ., Corvallis, 1973.

van de Hulst, H. C., *Light Scattering by Small Particles*, John Wiley, New York, 1957.

Voss, K. J., A spectral model of the beam attenuation coefficient in the ocean and coastal areas, *Limnol. Oceanogr.*, *37*, 501–509, 1992.

Zaneveld, J. R. V., Remotely sensed reflectance and its dependence on vertical structure: A theoretical derivation, *Appl. Opt.*, *21*, 4146–4150, 1982.

Zaneveld, J. R. V., A theoretical derivation of the dependence of the remotely sensed reflectance of the ocean on the inherent optical properties, *J. Geophys. Res.*, this issue.

Zaneveld, J. R. V., J. C. Kitchen, A. Bricaud, and C. Moore, Analysis of *in situ* spectral absorption meter data, Ocean Optics 11, *Proc. SPIE Int. Soc. Opt. Eng.*, *1750*, 187–200, 1992.

Zaneveld, J. R. V., J. C. Kitchen, and C. Moore, The scattering error correction of reflecting-tube absorption meters, Ocean Optics 12, *Proc. SPIE Int. Soc. Opt. Eng.*, *2258*, 44–55, 1994.

J. C. Kitchen and J. R. V. Zaneveld, College of Oceanic and Atmospheric Sciences, Oregon State University, Ocean Administration Building 104, Corvallis, OR 97331.

(Received April 7, 1994; revised September 21, 1994; accepted November 30, 1994.)